



University of
Zurich^{UZH}

Zurich Open Repository and
Archive

University of Zurich
University Library
Strickhofstrasse 39
CH-8057 Zurich
www.zora.uzh.ch

Year: 2016

Camphopyrazole-based N,N- and N,P-ligands and chiral complexes of Ni, Pd, and Rh: P–N bond activation upon Rh(I) complexation

Herrera, Alberto ; Briceño, Alexander ; Gonzalez, Teresa ; Linden, Anthony ; Heinemann, Frank W ; Agrifoglio, Giuseppe ; Pastrán, Jesús ; Dorta, Romano

Abstract: Enantiomerically pure C1 and C2-symmetric bidentate N,N- and N,P-ligands are accessible from (+)-camphor in good yields (60–90%). Modified syntheses of precursors 1 and 2 are disclosed as well as the crystal structures of three hydroxy-pyrazoline intermediates. Ligands 3, 4, 6, and 11 were fully characterized including an X-ray crystal structure of C2-symmetric 6, which showed an E-configuration in the solid state. These ligands form complexes with Ni(II), Pd(II), and Rh(I) in good yields (84–96%); the X-ray crystal structures of complexes 12, 14, and 16 confirmed the bidentate coordination modes of ligands 4, 6, and 11 and distorted tetrahedral [for Ni(II)] and square planar [for Rh(I)] coordination geometries. Furthermore, the structure of the Rh(I) complex 16 revealed the presence of a Ph₂PCl ligand, which, along with spectroscopic data, is proof of an almost quantitative P–N bond cleavage upon coordination of ligand 11 to [RhCl(COD)]₂.

DOI: <https://doi.org/10.1016/j.tetasy.2016.06.013>

Posted at the Zurich Open Repository and Archive, University of Zurich

ZORA URL: <https://doi.org/10.5167/uzh-125958>

Journal Article

Accepted Version



The following work is licensed under a Creative Commons: Attribution-NonCommercial-NoDerivatives 4.0 International (CC BY-NC-ND 4.0) License.

Originally published at:

Herrera, Alberto; Briceño, Alexander; Gonzalez, Teresa; Linden, Anthony; Heinemann, Frank W; Agrifoglio, Giuseppe; Pastrán, Jesús; Dorta, Romano (2016). Camphopyrazole-based N,N- and N,P-ligands and chiral complexes of Ni, Pd, and Rh: P–N bond activation upon Rh(I) complexation. *Tetrahedron: Asymmetry*, 27(16):759-767.

DOI: <https://doi.org/10.1016/j.tetasy.2016.06.013>

Camphopyrazole-Based N,N- and N,P-Ligands and Chiral Complexes of Ni, Pd, and Rh.

P–N Bond Activation upon Rh(I) Complexation

Alberto Herrera,¹ Alexander Briceño,³ Teresa Gonzalez,³ Anthony Linden,⁴ Frank W. Heinemann,¹
Giuseppe Agrifoglio,² Jesús Pastrán,*² Romano Dorta*¹

¹ *Department Chemie und Pharmazie, Anorganische und Allgemeine Chemie, Friedrich–Alexander–Universität Erlangen–Nürnberg, Egerlandstr. 1, 91058 Erlangen, Germany*

² *Departamento de Química, Universidad Simón Bolívar, Caracas 1080A, Venezuela,*

³ *Centro de Química, Instituto Venezolano de Investigaciones Científicas (IVIC), Miranda, Venezuela*

⁴ *Department of Chemistry, University of Zurich, Winterthurerstrasse 190, CH-8057, Zurich, Switzerland*

Correspondence e-mail: jpastran@usb.ve, romano.dorta@fau.de

Abstract

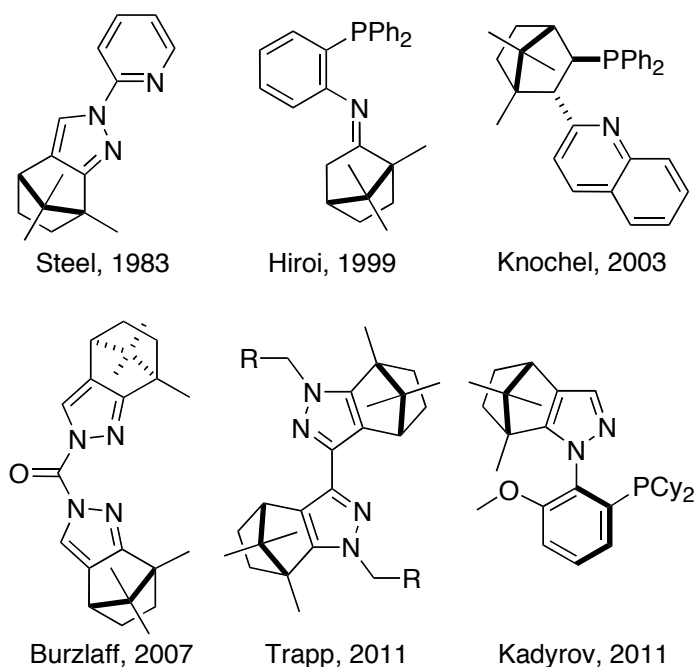
Optically pure C_1 and C_2 -symmetric bidentate N,N and N,P ligands are accessible from (+)-camphor in good yields (60-90%). Modified syntheses of precursors **1** and **2** are disclosed as well as the crystal structures of three hydroxy-pyrazoline intermediates. Ligands **3**, **4**, **6**, and **11** were fully characterized including an X-ray crystal structure of C_2 -symmetric **6** showing an *E* configuration in the solid state. These ligands form complexes with Ni(II), Pd(II), and Rh(I) in good yields (84-96%), and the X-ray crystal structures of complexes **12**, **14**, and **16** confirm bidentate coordination modes of ligands **4**, **6**, and **11** and distorted tetrahedral (for Ni(II)) and square planar (for Rh(I)) coordination geometries. Furthermore, the structure of the Rh(I) complex **16** revealed the presence of a PPh_2Cl ligand, which, along with spectroscopic data, is proof of an almost quantitative P–N bond cleavage upon coordination of ligand **11** to $[\text{RhCl}(\text{COD})]_2$.

Keywords: Camphopyrazole; Chiral N,N- and N,P-ligands; 3-hydroxypyrazolines; Ni(II)-, Pd(II)-, and Rh(I) complexes; P–N activation; (+)-camphor; hydroxy-pyrazolines

1. Introduction

The design and synthesis of new chiral ligands and complexes play an important role in the development of asymmetric catalysis. For over three decades, camphor has been used as an easily modifyable and inexpensive building block from the chiral pool for the synthesis of C_1 , C_2 , and C_3 symmetric ligands.¹ In particular, the campho[2,3-*c*]pyrazole motif² was introduced in the 1980s by Steel and co-workers as a new design element for chiral N-donor ligands,³ and more recently, Trapp *et al.* prepared bipyrazole-camphor derived C_2 -symmetric ligands for Pd-catalyzed Wacker oxidations and alkene isomerizations.⁴ In contrast, camphor-derived P,N ligands⁵ are less common even though chiral P,N ligands such as QUINAP⁶ are widely used in asymmetric catalysis.⁷ The success of such ligands in asymmetric catalysis is in part due to the hemilability of the N function and in part to the synergism between the soft, π -accepting P donor that stabilizes low-valent metal centers, and the hard N σ -donor that renders the metal more susceptible to oxidative addition reactions. This combination not only stabilizes intermediate oxidation states during a catalytic cycle, but the electronic dissymmetry also provides stereocontrol due to distinguishing *trans* influences of the P and N donors.

Chart 1. Selected examples of camphor-derived N–N and N–P ligands



Herein we report the syntheses of new camphopyrazole-based N,N ligands with C_1 and C_2 symmetry and a P-N ligand that resembles QUINAP electronically and in its bite angle. Along these multi-step syntheses several intermediates are characterized fully for the first time. We show that the new ligands

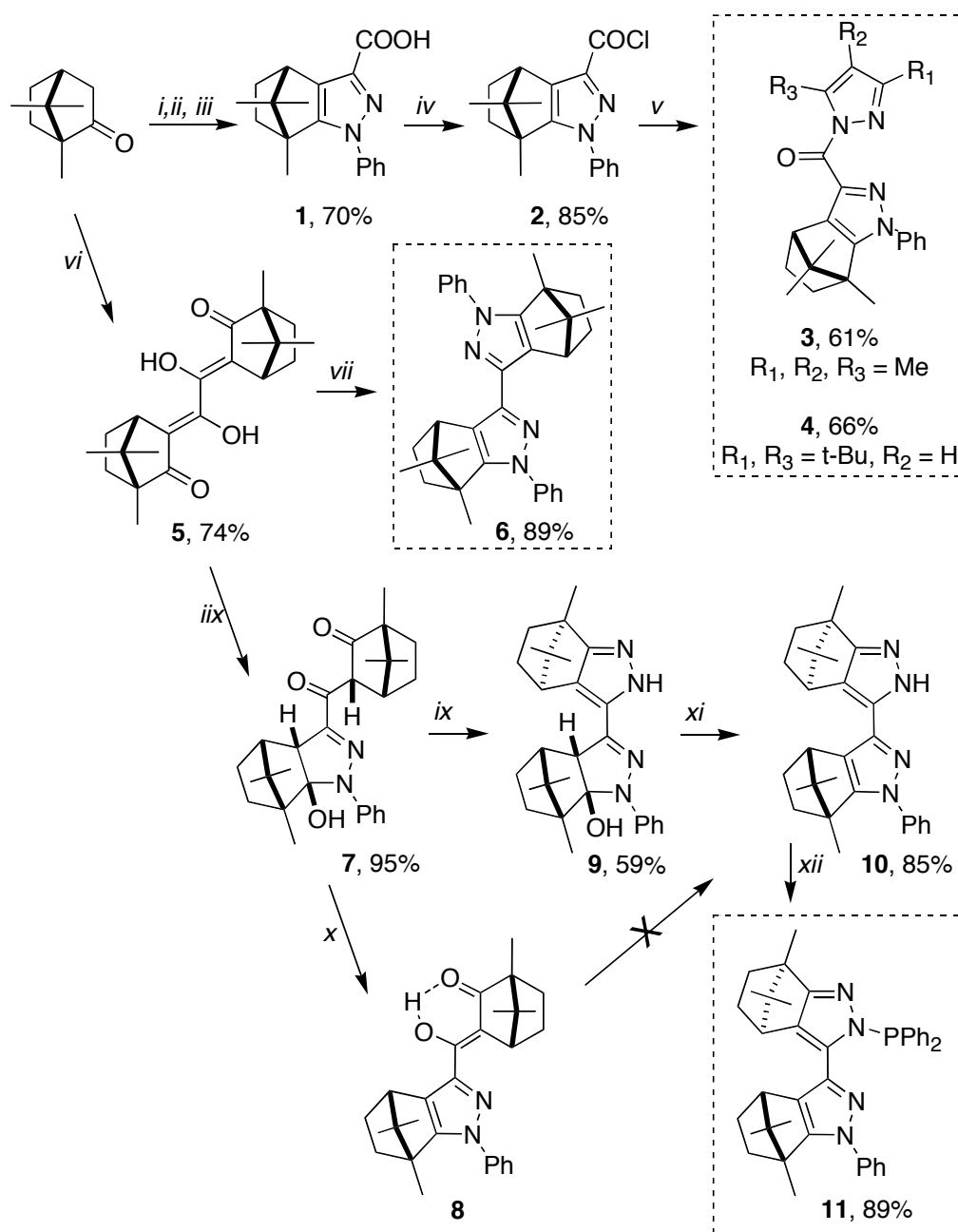
form bidentate coordination compounds with Ni(II), Pd(II), and Rh(I), affording chiral complexes with catalytic potential.⁸ We also disclose a mild and selective P–N bond activation that takes place upon coordination of the P,N ligand **11** to a Rh(I) chloride precursor.

2. Syntheses and structures of intermediates and ligands

Ligands **3**, **4**, **6**, and **11** were prepared starting from (+)-camphor according to Scheme 1. Compound **1**⁹ was obtained in good yield by a modified procedure that minimized the formation of by-products.¹⁰ The X-ray crystal structure of **1** is depicted in Figure 1 and shows the two molecules of the asymmetric unit, which are linked *via* non-centrosymmetric hydrogen bonds between carboxylic acid groups. While the carboxylic acid functions are approximately co-planar with the pyrazole rings, the phenyl rings are not: The N1–N2–C5–C10 and N3–N4–C23–C24 torsion angles are $-47.8(7)^\circ$ and $36.6(7)^\circ$, respectively.

The acyl chloride **2** was obtained in good yield by refluxing **1** in SOCl₂ and recrystallizing the crude product from heptane,¹¹ and ligand **3** was obtained in acceptable yield by reacting the corresponding pyrazole with **2** in the presence of NEt₃. For ligand **4**, in contrast, it was necessary to first generate the sodium-3,5-di-*tert*-butyl-pyrazolate anion *in situ* in order to ensure sufficient reactivity with **2**. The reaction is favored by the formation of NaCl and yields up to 66% of **4**. Characteristic ¹H NMR resonances of **2**, **3** and **4** corresponding to the bridgehead protons are found at 3.21 ppm, 2.90 ppm, and 2.77 ppm, respectively, and the corresponding ¹³C resonances of the carbonyl groups are all similar at around 162–163 ppm. A modified procedure allowed us to isolate compound **5**¹² on a 30-gram scale in good yields and excellent purity. Our method is characterized by an easier purification step that affords a product with a significantly higher and sharper melting point (228–230 °C *vs.* 178–186 °C).⁴ Finally, the C₂-symmetric ligand **6** was isolated in very good yield after acid-catalyzed condensation of phenyl hydrazine with **5** in refluxing ethanol. Its precise molecular structure was determined by a single crystal X-ray diffraction analysis. Figure 2 shows the approximate C₂ point symmetry and *E* configuration of the free ligand **6**, characterized by a N2–C1–C18–N4 torsion angle of $175.5(5)^\circ$. The dihedral angles between the pyrazole rings and phenyl groups may conveniently be approximated by the N2–N1–C12–C13 and N4–N3–C30–C31 torsion angles, which are $-136.8(5)^\circ$ and $-49.2(7)^\circ$, respectively.

Scheme 1. Syntheses of (+)-camphor-based N,N and N,P ligands **3**, **4**, **6**, and **11**.



(i) Diethyl oxalate, NaH, THF; (ii) KOH, EtOH; (iii) PhNHNH₂, H₂SO₄, EtOH, reflux; (iv) SOCl₂, reflux; (v) for **3**: 3,4,5-trimethylpyrazol, NEt₃, acetone; for **4**: 3,5-di-tert-butylpyrazol, Na, THF; (vi) diethyl oxalate, NaH, THF, reflux; (vii) PhNHNH₂, HCl, EtOH, reflux; (iix) PhNHNH₂, AcOH, EtOH, reflux; (ix) hydrazine hydrate, AcOH, EtOH, reflux; (x) hydrazine sulfate; (xi) HCl (conc), THF; (xii) 1. LDA, -28 °C to RT, 2. PCIPh₂, THF.

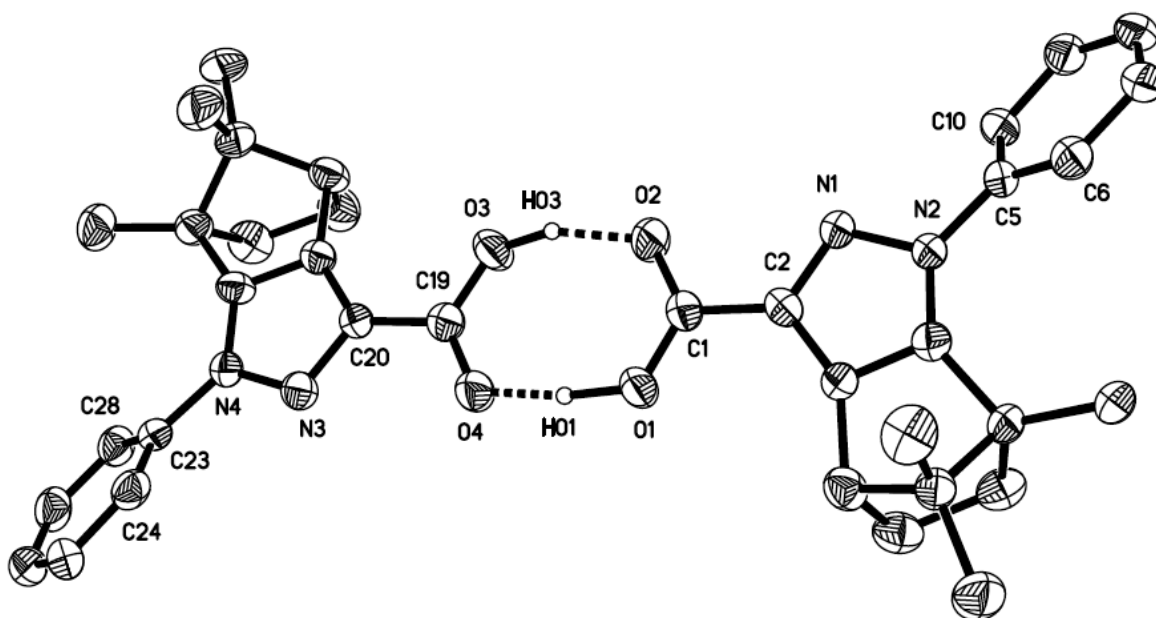


Figure 1. ORTEP representation (30% displacement ellipsoids) of both independent molecules of **1** in the crystal, showing the non-centrosymmetric, hydrogen-bonded dimer. Most H atoms are omitted. Selected bond lengths (Å) and angles (°) are: N1–N2 1.373(5), N2–C5 1.413(6), C1–C2 1.462(7), C1–O1 1.263(6), C1–O2 1.267(7), N3–N4 1.352(5), N3–C20 1.347(6), N4–C23 1.453(6), C19–O3 1.284(6), C19–O4 1.251(7), C5–N2–N1 117.2(4), C2–N1–N2 105.0(4), N1–C2–C1 120.3(5), O1–C1–O2 123.7(5), N3–N4–C23 118.0(4), C20–N3–N4 104.8(4), N3–C20–C19 118.9(5), O3–C19–O4 122.6(5), N3–N4–C21 111.5(4).

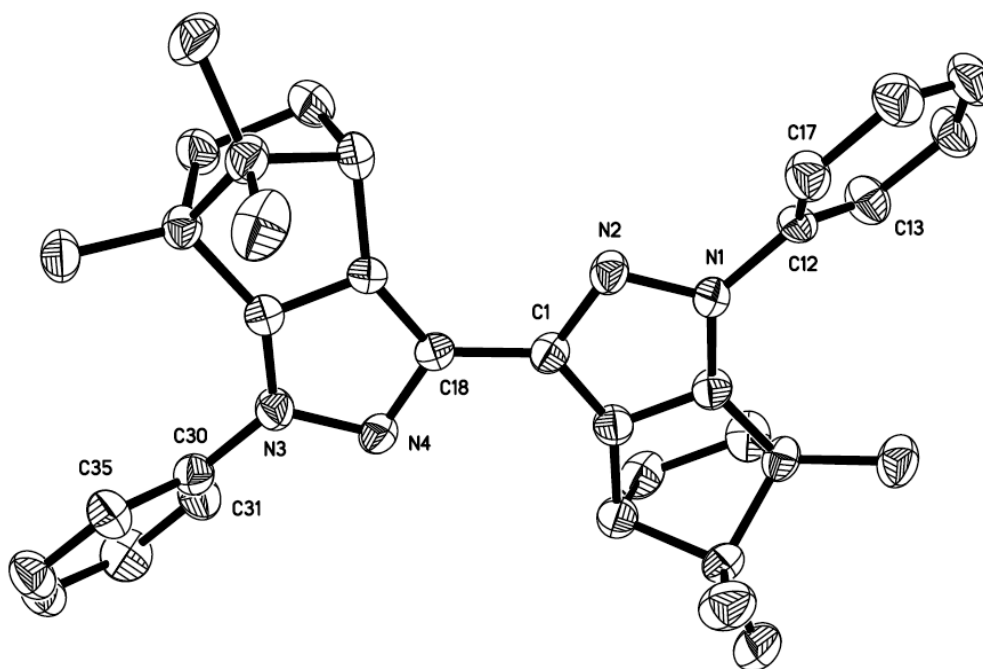


Figure 2. ORTEP representation (30% displacement ellipsoids) of **6** in the crystal. H atoms are omitted. Selected bond lengths (Å) and angles (°) are: N1–N2 1.379(5), N1–C12 1.427(6), C1–C18 1.464(6), N3–N4 1.381(5), N4–C18 1.354(6), N1–N2–C1 104.5(4), N2–N1–C12 118.1(4), N3–N4–C18 103.8(4), N4–N3–C30 118.7(4), N4–C18–C1 119.3(4), N2–C1–C18 118.8(4).

The hydrated pyrazole **7** was prepared in almost quantitative yield. Its molecular structure was established by single crystal X-ray crystallography and confirms three important features (see Figure 3): (i) a *trans*-configuration about C1–C18, which also implies that the camphor moieties are in *trans* positions to each other, (ii) a preference for the diketo tautomer, and (iii) the presence of a hydroxy pyrazole ring. The attempted condensation of diketone **7** with hydrazine sulfate only lead to the dehydration and tautomerization of **7** affording the keto-enol pyrazole **8**. Its crystal structure again shows a *trans* configuration of the C17–C18 bond and the camphor units (Figure 4). Our target molecule **10** could not be obtained by condensation of hydrazine with **8** under varying conditions, but the condensation of **7** with hydrazine produced **9**, which was dehydrated in refluxing THF in the presence of HCl to afford **10** in very good yields. The X-ray crystal structure of **9** (Figure 5), which crystallized as a hemihydrate, reveals two interesting features: it maintains the hydrated phenyl substituted pyrazole ring, and the presence of the second H-substituted pyrazole ring forces a *cis*-configuration of the molecule, probably thanks to the H-bonding to N2. Finally, *in situ* deprotonation of **10** with LDA at -28 °C, followed by reaction with PPh₂Cl and washing with hexane afforded the P-N ligand **11** as a white powder in good yield. The ³¹P NMR spectrum shows a singlet at 45.9 ppm that remained unchanged after heating at 45 °C for 2 h.¹³ The structure of **11** was confirmed in a Rh complex (*vide infra*).

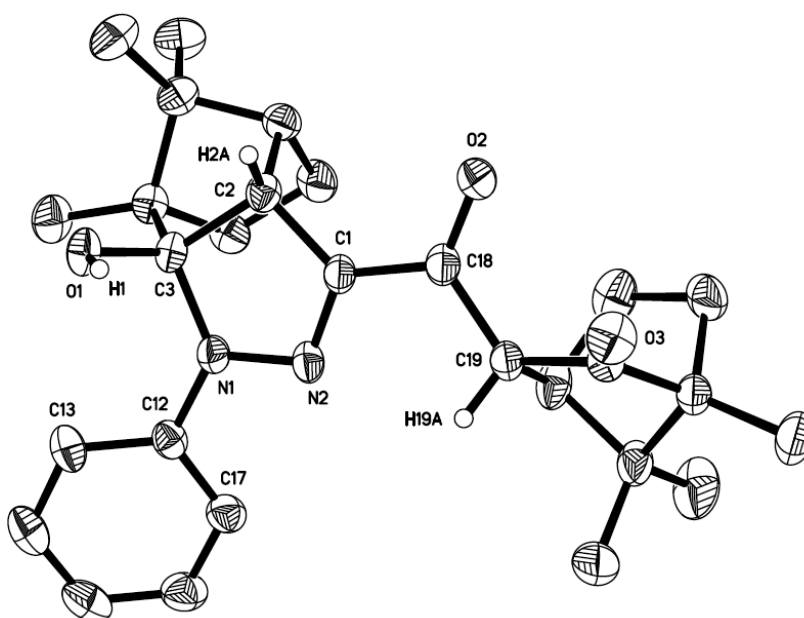


Figure 3. ORTEP representation (30% probability ellipsoids) of one of the two independent molecules of **7** in the crystal. Most H atoms are omitted. Selected bond lengths (Å) and angles (°) are: C1–N2 1.308(4), N1–N2 1.361(4), N1–C12 1.413(4), N1–C3 1.500(4), C3–O1 1.394(4), C18–O2 1.235(4), C24–O3 1.210(4), C18–C19 1.501(5), C1–N2–N1 109.4(3); N2–N1–C12 117.3(3); N2–C1–C2 113.6(3); O2–C18–C1 120.3(3); O2–C18–C19 122.6(3), C18–C1–C2 127.5(3), O1–C3–N1 110.0(3), O3–C24–C19 125.5(3).

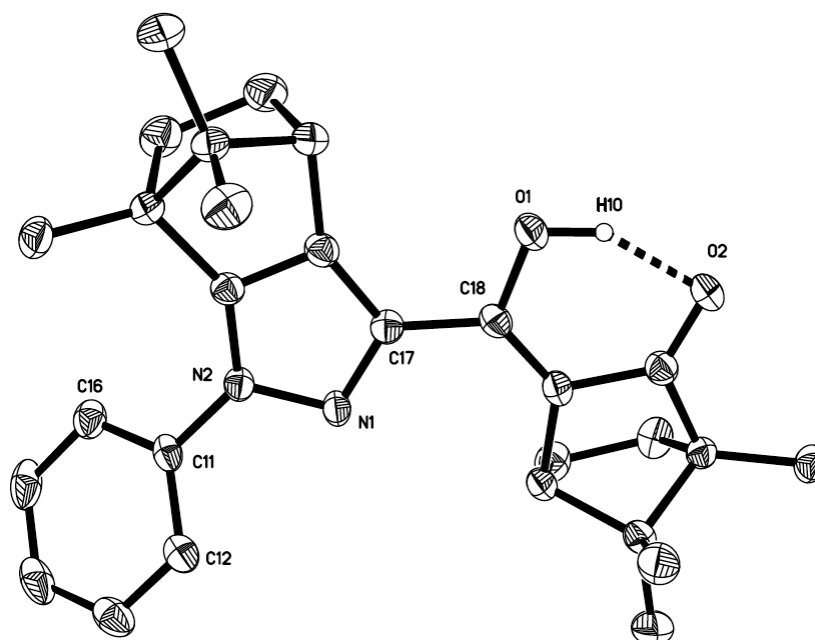


Figure 4. ORTEP representation (50% probability ellipsoids) of one of the two independent molecules of **8** in the crystal. Most H atoms are omitted. Selected bond lengths (Å) and angles (°) are: O1–C18 1.353(3), O2–C20 1.243(3), N1–C17 1.344(3), N1–N2 1.368(3), N2–C1 1.362(3), N2–C11 1.422(3), C1–C2 1.358(3), C2–C17 1.394(3), C17–C18 1.465(3), C18–C19 1.350(3), C19–C20 1.454(3), N2–C1–C6 143.1(2), C17–C2–C3 146.7(2), O1–C18–C17 111.6(2).

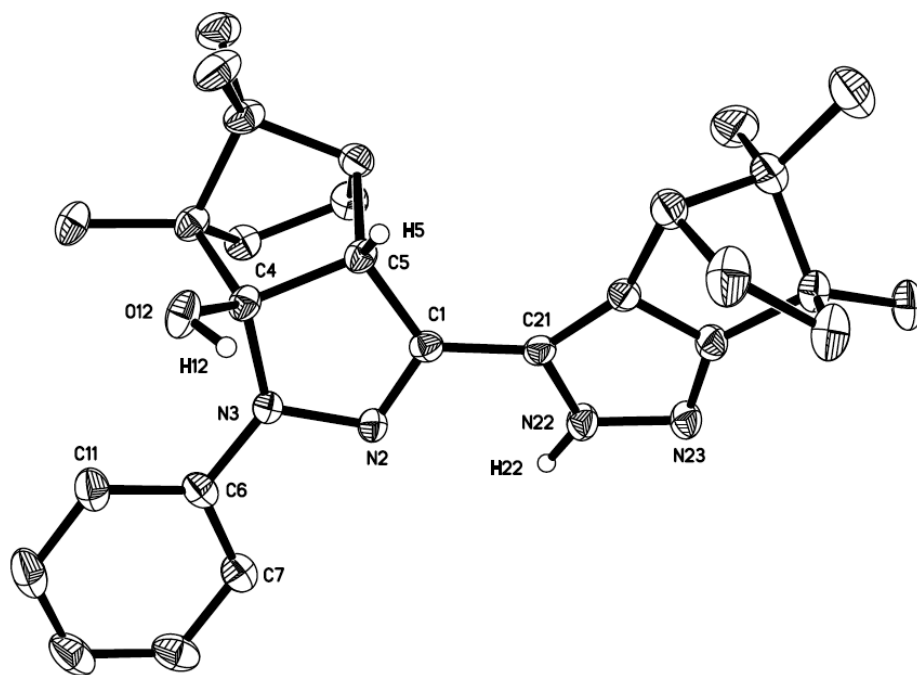


Figure 5. ORTEP representation (50% probability ellipsoids) of one of the two independent molecules of **9** in the crystal. Most H atoms are omitted. Selected bond lengths (Å) and angles (°) are: C1–C5 1.489(2), N2–C1 1.292(2), N2–N3 1.373(2), N3–C4 1.482(2), C4–C5 1.570(2), O12–C4 1.405(2), C1–C21 1.451(2), N22–C21 1.371(2), N22–N23 1.357(2), N23–C24 1.323(2), C24–C25 1.394(2), C21–C25 1.377(2), O12–C4–N3 110.4(1), O12–C4–C5 114.9(1), C1–C5–C4 102.2(1).

3. Complexes of Nickel, Palladium, and Rhodium

Ligands **3**, **4** and **6** were then reacted with $\text{NiBr}_2(\text{THF})_2$ ¹⁴ in THF solution at room temperature to afford complexes **12**, **13** and **14**, respectively, in very good isolated yields (Scheme 2). These complexes are air-stable for a few hours and display low solubilities in hydrocarbon solvents. Although the paramagnetic nature of complexes **12–14**, precluded a meaningful NMR characterization, elemental analyses are satisfactory, and single crystal X-ray diffraction analyses of **12** and **14** confirm their structures. Complex **15** was obtained from $\text{PdCl}_2(\text{CH}_3\text{CN})_2$ ¹⁵ and ligand **6** in THF solution. The complex is air-stable and highly soluble in common organic solvents. The ¹H NMR spectrum shows a slight but characteristic low frequency shift of 0.05 ppm of the bridge-head protons when compared to the free ligand.

One of the two symmetry independent molecules of **12** is depicted in Figure 4. In both of them the tetrahedral coordination geometry is distorted as a result of the small bite angle of the ligand of around 90°, which is compensated by an increase of the Br–Ni–Br angles to about 125°. In both molecules, the ligand is coordinated to the nickel atom through the available N atoms forming a six-membered planar chelation ring. The Ni–N and Ni–Br bond distances in **12** are slightly shorter than the ones observed in

similar nickel complexes with six-membered chelate rings.^{16,17} The dihedral angles between the pyrazole rings and phenyl groups may be conveniently approximated by the N1–N2–C13–C14 and N7–N8–C36–C37 torsion angles, which are 66.6(13)° and -65.8(9)°, respectively.

Chart 2. The Ni(II) and Pd(II) complexes **12–15**

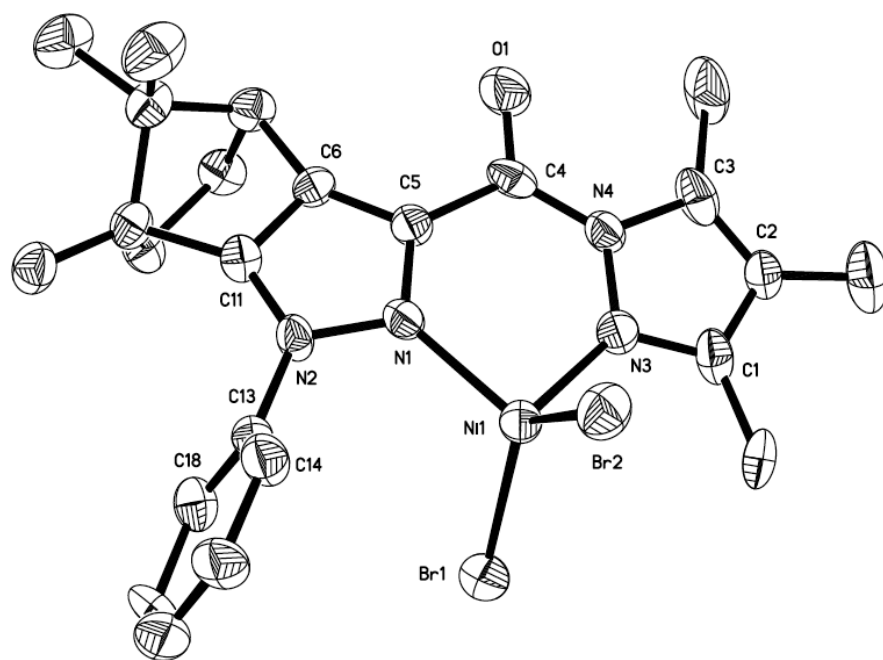
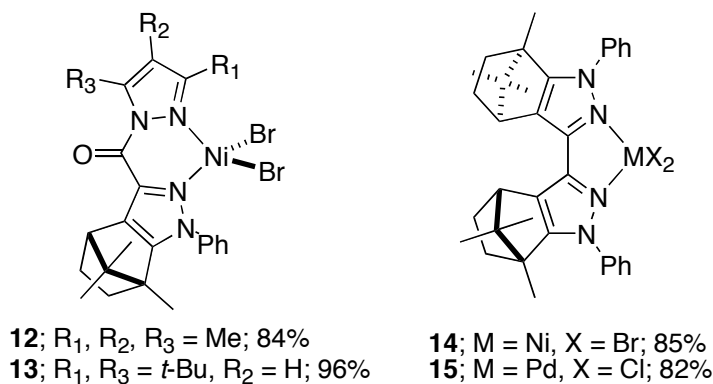


Figure 4. ORTEP view (30% displacement ellipsoids) of one of the two independent molecules of **12** in the crystal. H atoms are omitted. Selected bond lengths (Å) and angles (°) are: N1–Ni1 1.968(10), N3–Ni1 1.979(10), Ni1–Br1 2.348(3), Ni1–Br2 2.358(2), O1–C4 1.204(14), C4–N4 1.383(15), C4–C5 1.494(14), Br1–Ni1–Br2 125.38(8), N1–Ni1–N3 89.5(4), C5–N1–N2 105.8(8), N4–N3–C1 104.9(10).

Complex **14** also crystallized with two independent molecules in the asymmetric unit representing the same enantiomer but differing in the orientation of the phenyl rings (Figure 5). One of the bromine atoms in each of the independent molecules was disordered to a small extent. Two alternative

orientations were refined for each molecule resulting in site occupancies of 0.949(2) and 0.051(2) for Br2 and Br2A and of 0.956(2) and 0.044(2) for Br3 and Br3A, respectively. The distorted tetrahedral coordination geometry around Ni shows Br–Ni–Br angles of 121°–122° (considering only the major occupied sites for the bromide ligands in each independent molecule) and narrow N–Ni–N bite angles of around 80°. The five-membered chelation ring, together with the pyrazole rings, form a roughly coplanar fused three ring system. The Ni–N bond distances are slightly longer than values found in similar nickel dibromide Schiff-base complexes with five-membered chelate rings.^{14, 16} The N1–C3–C4–N3 torsion angle of the backbone is 2.5(5)° (6.9(5)° for the other independent molecule). The dihedral angles between the planes described by the phenyl groups and pyrazole rings are around 50° (see the corresponding torsion angles in the caption to Figure 5; for the second molecule the values are 41.0(5)° and 54.9(5)°).

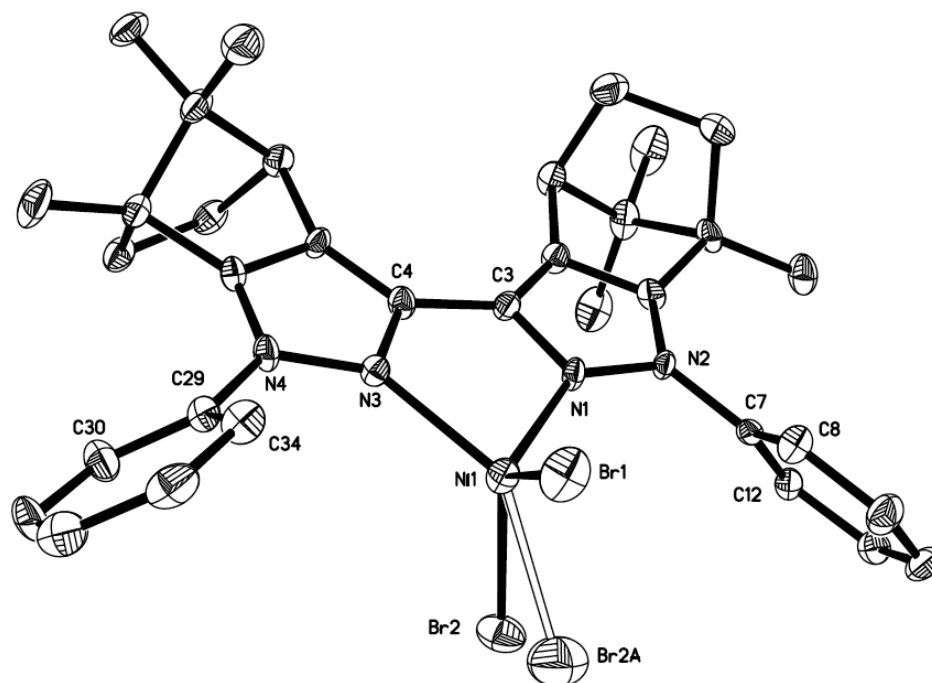
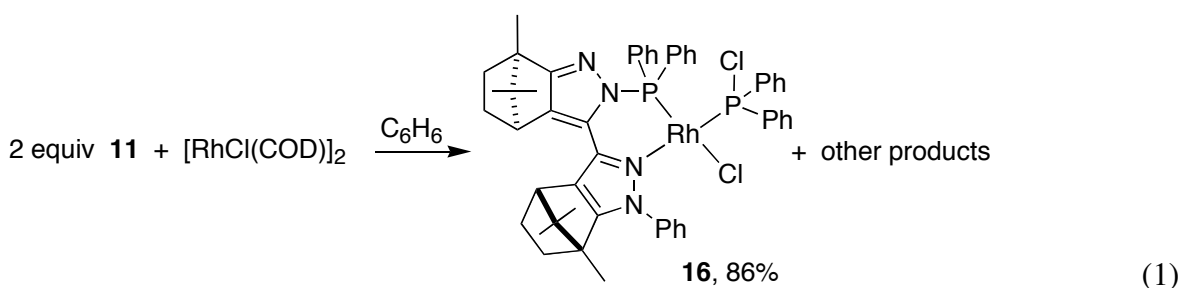


Figure 5. ORTEP view (50% displacement ellipsoids) of one of the two independent molecules of **14** in the crystal. H atoms are omitted. Selected bond lengths (Å) and angles (°) are: Ni1–N1 2.015(3), Ni1–N3 2.082(3), Ni1–Br1 2.3569(7), Ni1–Br2 2.3468(8), N1–N2 1.367(4), N1–C3 1.372(5), N2–C1 1.357(5), N3–C4 1.344(5), N3–N4 1.376(4), N4–C6 1.357(5), C1–C2 1.374(5), C2–C3 1.385(5), C3–C4 1.445(5), C4–C5 1.385(5), C5–C6 1.374(5), N3–Ni1–N1 80.4(1), Br1–Ni1–Br2 120.79(3), N1–N2–C7–C8 53.7(5), N3–N4–C29–C34 50.2(5).

Finally, two equivalents of ligand **11** were added dropwise to a slurry of [RhCl(COD)]₂ (COD = 1,5-cyclooctadiene) in benzene according to eq 1. After washing the crude product with hexane, an orange

powder was isolated in good yield. The ^{31}P NMR spectrum showed two doublets of doublets centered at $\delta = 100.7$ ppm ($J_{\text{PRh}} = 195.0$ Hz, $J_{\text{PP}} = J_{\text{PP}'} = 41.2$ Hz) and 130.7 ppm ($J_{\text{PRh}} = 222.6$ Hz, $J_{\text{PP}'} = J_{\text{P}'\text{P}} = 40.2$ Hz). This suggested the presence of a Rh center bonded to two different P atoms, and the magnitude of the $J_{\text{PP}'}$ and J_{PP} coupling constants pointed at a *cis* isomer. This unexpected bonding situation was then elucidated by an X-ray crystal structure analysis, which revealed the presence of a PPh_2Cl ligand in complex **16** (Figure 6). The cleavage of the pyrazolylphosphine P–N bond in half of the equivalents of ligand **11** by half of the Rh–Cl functions present in the starting material $[\text{RhCl}(\text{COD})]_2$ ¹⁸ accounts for the presence of PPh_2Cl in complex **16**. Considering this reaction stoichiometry, the isolated yield of **16** is 86% based on chloride or phosphorus equivalents.¹⁹



The asymmetric unit contains two independent molecules of **16** having the same ligand chirality. The compound crystallized with one molecule of CH_2Cl_2 per formula unit. Both show distorted square planar coordination environments around the Rh atom and are linked by a slipped π - π stacking interaction between the phenyl groups attached to atoms P1 and P3. The distance between the centroids of the phenyl rings of 4.012(4) Å lies within the values reported for this type of interaction (3.0-4.6 Å).²⁰ Ligand **11** is indeed bidentate forming a six membered chelate ring in a distorted envelope conformation, with Rh being the envelope flap atom: Rh1 is 0.94(5) Å from the mean plane defined by atoms P1, N3, C4, C3 and N1 (rms deviation of 0.0352 Å) and Rh2 is 1.04(5) Å from the plane defined by atoms N5, C55, C56, N7, and P3 (rms deviation 0.047 Å). This conformation is helped by the fact that all N atoms are almost perfectly trigonal planar, while the pseudo tetrahedral P1 atom pushes the Rh center out of plane. As anticipated by NMR spectroscopy, the other P ligand is in a *cis* position and turns out to be chlorodiphenylphosphine. The fact that the *cis* isomer is observed exclusively may be rationalized by the above mentioned strongly directing *trans*-influence exerted by P,N ligands. The chlorine atom Cl2 of the PPh_2Cl ligand stands roughly *anti* to the chloride ligand Cl1 with a Cl1–Rh1–P2–Cl2 torsion angle of $-159.03(5)^\circ$ ($156.81(5)^\circ$ for the second molecule). The Rh–N, Rh–P and Rh–Cl bond lengths lie within expected values.²¹ The N1–C3–C4–N3 and N5–C55–C56–N7 torsion angles in

the bis-pyrazole moieties of the two molecules measure $14.9(5)^\circ$ and $17.1(4)^\circ$, respectively, and are much smaller than the value of 65° seen in QUINAP.²²

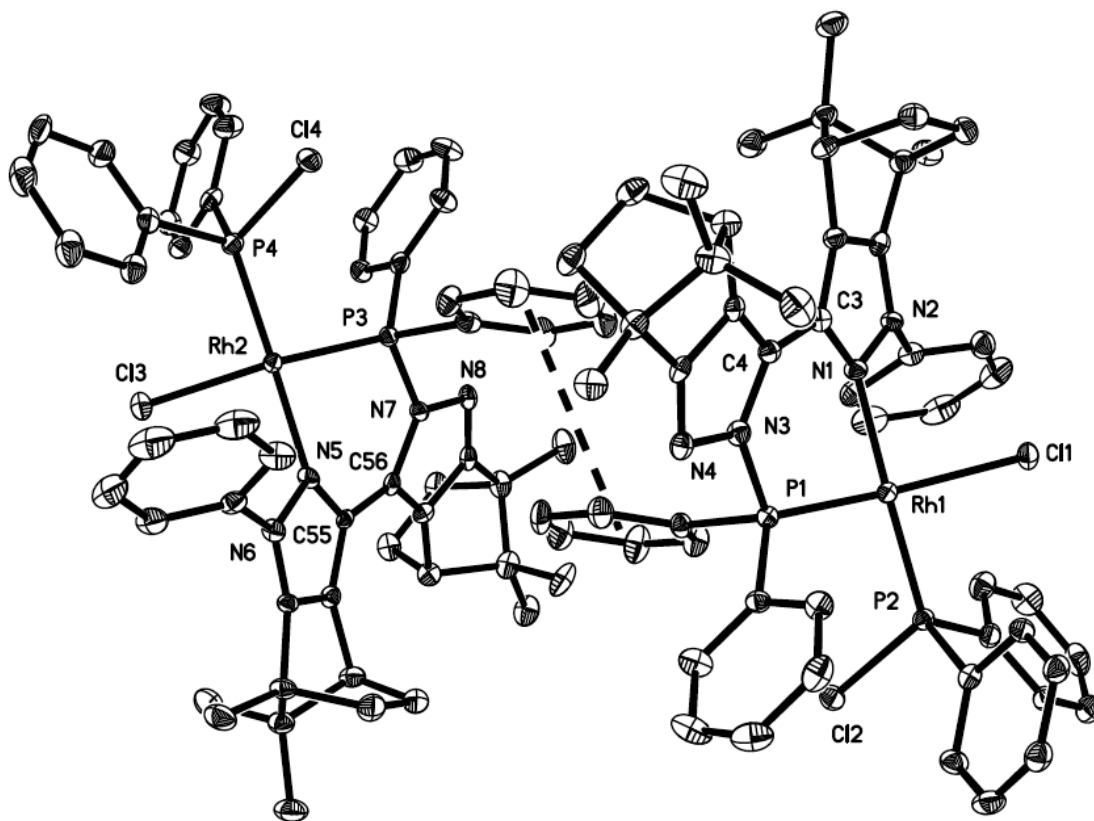


Figure 6. ORTEP view (50% displacement ellipsoids) of both independent molecules of **16** in the crystal, showing the slipped intermolecular π - π stacking interaction. H atoms are omitted. Selected distances (\AA) and angles ($^\circ$) are: Rh1–N1 2.100(3), Rh1–P1 2.1742(8), Rh1–P2 2.1835(9), Rh1–Cl1 2.3996(8), P1–N3 1.754(3), N3–C4 1.386(4), C4–C3 1.450(4), C3–N1 1.352(4), P2–Cl2 2.093(1), P1–N3–C4 128.3(2), N3–C4–C3 125.0(3), N1–C3–C4 121.5(3), Rh1–P1–N3 108.72(9), N1–Rh1–P1 88.75(8), P2–Rh1–P1 95.93(3), Cl1–Rh1–P2 88.31(3), N1–Rh1–Cl1 89.27(8).

4. Conclusion

Optically pure (+)-camphor-derived building blocks and C_1 and C_2 -symmetric N,N and N,P ligands are readily accessible in gram quantities and good yields. Important intermediates, notably hydroxypyrazolines, can also be isolated in good yields. The X-ray crystal structures of the free ligands and their Ni(II) complexes confirm the expected coordination modes and geometries. The P,N ligand **11** proved to possess a reactive P–N bond with respect to $[\text{RhCl}(\text{COD})]_2$, which is readily cleaved in the presence of the Rh(I)–Cl function. The structural evidence of this reactivity indicates that phosphine ligands with pyrazolyl- or imidazolyl-P–N bonds are not compatible with metal-halogenide precursors, and that non-halogen counter anions should be employed in order to avoid P–N activation.

Complexes **12–16** are being tested as homogeneous catalysts in different organic transformations and results will be reported in due course.

5. Experimental

General considerations: All reactions with air-sensitive compounds were carried out under anaerobic and anhydrous conditions, using standard Schlenk and glove box techniques. THF and Et₂O were distilled under nitrogen from purple Na/Ph₂CO solutions; pentane and hexanes from Na₂K alloy; CH₂Cl₂ from CaH₂. NMR spectra were recorded on a Jeol 400 MHz spectrometer. Optical rotations were measured on a Perkin-Elmer 241 polarimeter, and values of *c* are in g/100mL. Elemental analyses were performed at IVIC, samples were handled in air, and hygroscopic compounds are corrected for water content. Melting points were measured in sealed capillary tubes and are uncorrected. Commercial NaH as 60 % w/w dispersion in mineral oil was used as received. Ethyl formate was dried over CaH₂, fractionally distilled, and kept over activated MS 4 Å. Ethyl camphor-oxalate,²³ camphor-oxalic acid,²³ LDA,²⁴ NiBr₂(THF)₂,¹⁴ PdCl₂(CH₃CN)₂,¹⁵ and [RhCl(COD)]₂²⁵ were prepared following reported procedures.

(4S,7R)-7,8,8-trimethyl-4,5,6,7-tetrahydro-4,7-methano-1-phenylindazol-3-carboxylic acid (1): Concentrated H₂SO₄ (1.0 mL) was added slowly to a solution of (+)-camphor-oxalic acid (8.74 g, 38.9 mmol) in ethanol (50 mL) and the mixture was stirred for 15 min. Then a solution of phenyl-hydrazine (6.45 g, 59.6 mmol) in ethanol (30 mL) was added dropwise and the mixture heated to reflux overnight. Then the solvent was evaporated and the crude product dissolved in 3.0 M KOH (500 mL). The mixture was filtered and the filtrate acidified with 3.0 M HCl to precipitate the product, which was filtered off and dried *in vacuo*. Recrystallization from dichloromethane-hexane (1:1) and HV-drying afforded a yellow solid (7.95 g, 70 %). Mp 152-154 °C. $[\alpha]_D^{20} = +72.4$ (*c* 1.021, CHCl₃). ¹H-NMR (400 MHz, CDCl₃): δ 0.79 (s, 3H), 0.93 (s, 3H), 1.11 (s, 3H), 1.20-1.35 (m, 2H), 1.86-1.89 (m, 1H), 2.13-2.16 (m, 1H), 3.16-3.17 (d, *J*_{H-H} = 4 Hz, 1H), 5.43 (s, 1H), 7.35-7.47 (m, 5H). ¹³C {¹H} NMR (101 MHz, CDCl₃): δ 11.98, 19.63, 20.37, 27.20, 33.70, 47.95, 54.04, 63.91, 124.81 (2), 128.62, 128.99 (2), 133.76, 136.20, 139.39, 155.96, 166.86. Elemental analysis calculated for C₁₈H₂₀N₂O₂ (%): C, 72.95; H, 6.80; N, 9.45. Found: C, 72.70; H, 7.12; N, 9.33. X-ray-quality single crystals were obtained by vapor diffusion of hexane into a saturated dichloromethane solution of **1** and cooling to -10 °C for 2 d.

(4S,7R)-7,8,8-trimethyl-4,5,6,7-tetrahydro-4,7-methano-1-phenyl-indazol-3-carbonyl chloride (2): **1** (1.00 g, 3.37 mmol) was dissolved in SOCl₂ (10 mL) and heated under reflux for 3 h. After this time, excess SOCl₂ was evaporated under vacuum and the residue recrystallized from a dichloromethane-

hexane mixture (1:5). Drying *in vacuo* for 4 h afforded 0.90 g (85%) of a beige solid. Mp 140-142 °C (d). $[\alpha]_D^{20} = +59.1$ (c 0.305, CHCl₃). ¹H-NMR (400 MHz, CDCl₃): δ 0.79 (s, 3H), 0.93 (s, 3H), 1.12 (s, 3H), 1.25-1.35 (m, 2H), 1.88-1.92 (m, 1H), 2.16-2.19 (m, 1H), 3.21-3.22 (d, $J_{H-H} = 4$ Hz, 1H), 7.47-7.55 (m, 5H). ¹³C {¹H} NMR (101 MHz, CDCl₃): δ 11.85, 19.56, 20.34, 27.00, 33.60, 48.78, 54.22, 63.93, 124.85 (2), 129.17 (3), 134.88, 139.09, 139.52, 156.57, 161.98. Elemental analysis calculated for C₁₈H₁₉ClN₂O·H₂O (%): C, 64.96; H, 6.36; N, 8.42. Found: C, 64.39; H, 5.88; N, 8.41.

((4S,7R)-7,8,8-trimethyl-4,5,6,7-tetrahydro-4,7-methano-1-phenyl-indazol-3-yl)(3,4,5-trimethylpyrazol-1-yl)methanone (3): A solution of NEt₃ (285 mg, 2.81 mmol) in acetone (10 mL) was added to a solution of 3,4,5-trimethylpyrazole (310 mg, 2.81 mmol) in acetone (20 mL). The mixture was stirred for 15 min and then added to a solution of **2** (886 mg, 2.81 mmol) in acetone (20 mL). After heating to reflux for 5 h, the mixture was filtered and the solvent removed under vacuum. The resulting solid was washed and slurried in heptane (5x10 mL) and HV-dried to give 665 mg (61%) of a beige powder. Mp 201-202 °C. $[\alpha]_D^{20} = +46$ (c 0.21, THF). ¹H-NMR (400 MHz, CDCl₃): δ 0.77 (s, 3H), 0.89 (s, 3H), 1.10 (s, 3H), 1.47-1.49 (m, 1H), 1.59-1.60 (m, 1H), 1.86-1.93 (m, 1H), 1.93 (s, 3H), 2.10-2.19 (m, 1H), 2.19 (s, 3H), 2.54 (s, 3H), 2.90-2.91 (d, $J_{H-H} = 4$ Hz, 1H), 7.34-7.52 (m, 5H). ¹³C {¹H} NMR (101 MHz, CDCl₃): δ 7.75, 12.12, 12.33, 12.51, 19.80, 20.41, 26.89, 34.01, 50.31, 53.73, 63.26, 117.33, 124.89 (2), 128.24, 128.82 (2), 133.54, 139.03, 139.68, 140.06, 152.13, 154.40, 162.50. Elemental analysis calculated for C₂₄H₂₈N₄O·0.5H₂O (%): C, 72.52; H, 7.35; N, 14.09. Found: C, 72.32; H, 7.11; N, 13.92.

((4S,7R)-7,8,8-trimethyl-4,5,6,7-tetrahydro-4,7-methano-1-phenyl-indazol-3-yl)(3,5-di-*tert*-butylpyrazol-1-yl)methanone (4): Na (0.23 g, 10 mmol) was added to a solution of 3,5-di-*tert*-butylpyrazole (1.05 g, 5.84 mmol) in THF (40 mL) and stirred at RT for 18 h. Then the mixture was filtered and added to a solution of **2** (1.50 g, 4.76 mmol) in THF (15 mL) and stirred at RT for 10 h. After evaporating the solvent under vacuum, the crude product was dissolved in heptane (30 mL), filtered, and the solvent removed under vacuum to afford a beige powder (1.44 g, 66 %). Mp 144-145 °C. $[\alpha]_D^{20} = +47$ (c 0.06, THF). ¹H-NMR (400 MHz, CDCl₃): δ 0.83 (s, 3H), 0.86 (s, 3H), 1.10 (s, 3H), 1.35 (s, 9H), 1.30-1.50 (m, 2H), 1.44 (s, 9H), 1.83-1.86 (m, 1H), 2.00-2.06 (m, 1H), 2.76-2.78 (d, $J_{H-H} = 4$ Hz, 1H), 6.16-6.17 (s, 1H), 7.39-7.53 (m, 5H). ¹³C {¹H} NMR (101 MHz, CDCl₃): δ 12.15, 19.75, 20.44, 27.72, 30.01 (3), 30.26 (3), 32.45, 33.22, 33.78, 49.22, 53.66, 63.29, 105.85, 124.89 (2), 128.32, 128.82 (2), 133.61, 139.67, 139.85, 154.31, 157.29, 162.85, 163.00. Elemental analysis calculated for C₂₉H₃₈N₄O·1/2H₂O (%): C, 74.48; H, 8.41; N, 11.98. Found: C, 74.14; H, 8.08; N, 11.68.

(+)-(1R,1'R)-3,3'-(1,2-Dihydroxyethane-1,2-diylidene)bis[(1,7,7-trimethyl-bicyclo[2,2,1]-heptan-2-one] (5): A mixture of (+)-camphor (36.5 g, 0.240 mmol) and diethyl oxalate (15.9 g, 0.109 mmol) in THF (300 mL) was added to a slurry of NaH (21.5 g, 60% dispersion in mineral oil, 0.54 mmol) in THF (100 mL). The mixture was refluxed for 48 h, after which the solvent was removed by rotary evaporation. The reaction crude was added to an ice/HCl mixture and extracted with chloroform (3 x 50 mL). The organic layer was dried with MgSO₄, filtered, and stripped to a yellow oil. Slurrying and washing with MeOH (3 x 50 mL) yielded 29.09 g (74%) of a yellow powder. Mp 228-230 °C. $[\alpha]_D^{20} = +520.8$ (c 1.02, CHCl₃). Elemental analysis calculated for C₂₂H₃₀O₄ (%): C, 73.71; H, 8.43. Found: C, 73.95; H, 8.76. ¹H NMR (400 MHz, CDCl₃): δ 0.82 (s, 3H), 0.91 (s, 3H), 0.97 (s, 3H), 1.40-1.46 (m, 2H), 1.46-1.69 (m, 1H), 1.72-2.04 (m, 1H), 3.26-3.27 (d, *J*_{H-H} = 4 Hz, 1H), 11.81 (s, 1H) ppm. ¹³C {¹H} NMR (101 MHz, CDCl₃): δ 8.86, 9.61, 18.65, 18.71, 20.54, 20.72, 26.04, 27.13, 30.53, 31.71, 47.97, 48.56, 49.00, 49.14, 57.95, 59.65, 120.70, 123.33, 155.34, 157.39, 211.59, 214.79.

(+)-3,3'-bi(1,1'-diphenyl-pyrazole-camphor) or (1,1'-diphenyl-7,7',8,8',8'-hexamethyl-4,4',5,5',6,6',7,7'-octahydro-3,3'-bi-4,7-methano-indazole) (6): HCl (12.0 M, 1.0 mL) was added dropwise to a solution of **5** (1.68 g, 4.69 mmol) in ethanol (30 mL). After stirring for 15 min a solution of phenyl-hydrazine (1.52 g, 14.0 mmol) in ethanol (20 mL) was added dropwise and the resulting mixture refluxed for 24 h. Then, the solvent was removed by filtration and the white solid dried *in vacuo* (1.74 g, 89 %). M.P.: 284-285 °C (d). $[\alpha]_D^{20} = +105.7$ (c 1.01, CHCl₃). ¹H NMR (400 MHz, CDCl₃): δ 0.85 (s, 3H), 0.94 (s, 3H), 1.16 (s, 3H), 1.32-1.41 (m, 2H), 1.84-1.87 (m, 1H), 2.12-2.15 (m, 1H), 3.05-3.06 (d, 1H, *J* = 4 Hz), 7.28-7.30 (t, 1H), 7.39-7.42 (t, 2H), 7.52-7.54 (d, 2H, *J*_{H-H} = 8 Hz). ¹³C {¹H} NMR (101 MHz, CDCl₃): δ 12.54, 19.93, 20.58, 27.61, 33.92, 48.06, 53.57, 63.34, 124.57 (2), 127.06, 128.61 (2), 129.08, 139.89, 140.40, 154.11. Elemental analysis calculated for C₃₄H₃₈N₄ (%): C, 81.24; H, 7.62; N, 11.15. Found: C, 81.49; H, 8.02; N, 11.05. Single crystals suitable for an X-ray diffraction study were obtained by cooling a saturated EtOH solution of **6** to -10 °C for 2 d.

(+)-3,3'-[(1,2-Dihydroxyethane-1,2-diylidene)(1,7,7-trimethyl-bicyclo[2,2,1]-heptan-2-one)]-(1-phenyl-camphopyrazo-5-ol) or (+)-3,3'-[(1,2-Dihydroxyethane-1,2-diylidene)(1,7,7-trimethyl-bicyclo[2,2,1]-heptan-2-one)]-((4'S,7'R)-7',8',8'-trimethyl-4',6',7'-trihydro-5'-ol-4',7'-methano-1'-phenyl-indazol) (7): Acetic acid (0.5 mL) was added dropwise to a solution of **5** (4.50 g, 12.5 mmol) in EtOH (80.0 mL) and allowed to react for 15 min. Then a solution of phenyl hydrazine (1.36 g, 12.5 mmol) in EtOH (20.0 mL) was added dropwise to the above mixture and refluxed overnight. The solid crude product was isolated by filtration, and recrystallization from methanol at low temperature (-10 °C) followed by HV drying yielded a yellow powder (5.33 g, 95 %). Mp 203-204 °C.

$[\alpha]_D^{20} = +228.6$ (c 1.01, CHCl_3). Elemental analysis calculated for $\text{C}_{28}\text{H}_{36}\text{N}_2\text{O}_3 \cdot \text{H}_2\text{O}$ (%): C, 72.07; H, 8.21; N, 6.00. Found: C, 71.90; H, 8.56; N, 5.67. ^1H NMR (400 MHz, CDCl_3): δ 0.70 (s, 3H), 0.75 (s, 3H), 0.85 (s, 3H), 1.08 (s, 3H), 1.12 (s, 3H), 1.19 (s, 3H), 1.12-1.19 (m, 3H), 1.31-1.65 (m, 4H), 1.71-1.82 (m, 1H), 2.20-2.21 (d, $J_{\text{H-H}} = 4$ Hz, 1H), 2.51 (s, 1H), 3.84-3.85 (d, $J = 4$ Hz, 1H), 4.26 (s, 1H), 7.01-7.02 (t, 1H), 7.25-7.27 (t, 2H), 7.54-7.56 (d, $J = 8$ Hz, 2H) ppm. ^{13}C $\{^1\text{H}\}$ NMR (101 MHz, CDCl_3): δ 9.57, 12.79, 18.91, 19.48, 20.32, 20.83, 22.11, 22.21, 29.38, 31.22, 46.54, 47.06, 48.84, 51.69, 54.84, 58.26, 59.12, 59.18, 107.35, 118.61 (2), 123.19, 128.71 (2), 142.62, 147.17, 192.13, 215.55. Single crystals suitable for an X ray analysis were obtained from a cold filtered solution of **7** in MeOH (100 mg in 2.0 mL, -10°C for two days).

(+)-(E)-3,3'-(1-phenyl-camphopyrazole-hydroxymethylene)-(1,7,7-trimethylbicyclo[2.2.1]-heptan-2-one) or (E)-3,3'-((4S,7R)-7,8,8-trimethyl-4,6,7-trihydro-5-ol-4,7-methano-1-phenyl-indazol-hydroxymethylene)-((+)-1',7',7'-trimethylbicyclo[2'.2'.1']-heptan-2'-one) (8**):** Hydrazine sulfate (600 mg, 4.61 mmol) and **7** (2.06 g, 4.60 mmol) were dissolved in EtOH and the mixture refluxed overnight. After this time, the precipitate was separated by filtration and dried *in vacuo* (1.05 g, 53 %). Elemental analysis calculated for $\text{C}_{28}\text{H}_{34}\text{N}_2\text{O}_2 \cdot 0.15\text{H}_2\text{O}$ (%): C, 77.62; H, 7.98; N, 6.47. Found: C, 77.49; H, 7.76; N, 6.42. $[\alpha]_D^{20} = +252$ (c 1.00, CHCl_3). ^1H NMR (101 MHz, CDCl_3): δ 0.82 (s, 3H), 0.87 (s, 3H), 0.91 (s, 3H), 0.92 (s, 3H), 0.99 (s, 3H), 1.15 (s, 3H), 1.20-1.25 (m, 1H), 1.30-1.35 (m, 1H), 1.44-1.52 (m, 2H), 1.67-1.72 (m, 1H), 1.81-1.86 (m, 1H), 2.02-2.06 (m, 1H), 2.10-2.15 (m, 1H), 3.08-3.09 (d, 1H), 3.36-3.37 (d, 1H), 7.33-7.37 (m, 1H), 7.42-7.49 (m, 4H), 12.13 (s, 1H) ppm. ^{13}C $\{^1\text{H}\}$ NMR (101 MHz, CDCl_3): $\delta = 8.93, 12.45, 18.89, 19.73, 20.43, 20.58, 27.02, 27.42, 31.18, 33.75, 47.97, 48.59, 49.63, 53.62, 58.07, 63.35, 114.91, 124.22, 127.70, 128.82, 132.16, 140.05, 140.53, 154.33, 156.57, 213.58$. Single crystals suitable for an X-ray analysis were obtained by slow evaporation of an Et_2O solution of **8**.

(+)-3,3'-(1-phenyl-camphopyrazo-5-ol)-(2H-camphopyrazole) or 3,3'-((4S,7R)-7,8,8-trimethyl-4,6,7-trihydro-5-ol-4,7-methano-1-phenyl-indazol)-((4'S,7'R)-7',8',8'-trimethyl-4',5',6',7'-tetrahydro-4',7'-methano-2'H-indazol) (9**):** AcOH (0.50 mL) was added dropwise to a solution of **7** (1.85 g, 4.30 mmol) in EtOH (80.0 mL) and allowed to react for 15 min. Then a solution of hydrazine hydrate (5.15 g, 160 mmol) in EtOH (20.0 mL) was added dropwise and the resulting mixture was refluxed overnight. After this time, the precipitate was separated by filtration and purified by column chromatography (Merck G60, CH_2Cl_2) to afford a white solid (0.95 g, 52%). Mp $204-205^\circ\text{C}$. $[\alpha]_D^{20} = +215.3$ (c 0.538, CHCl_3). Elemental analysis calculated for: $\text{C}_{28}\text{H}_{36}\text{N}_4\text{O} \cdot \frac{1}{2}\text{H}_2\text{O} \cdot \frac{1}{4}\text{CH}_3\text{OH}$ (%): C, 73.50;

H, 8.30; N, 11.93. Found: C, 73.22; H, 7.92; N, 12.14. ^1H NMR (400 MHz, CDCl_3): δ 0.55 (s, 3H), 0.80-0.88 (m, 1H), 0.90 (s, 3H), 0.92 (s, 3H), 0.98-1.18 (m, 4H), 1.20 (s, 3H), 1.21 (s, 3H), 1.25 (s, 3H), 1.28-1.50 (m, 2H), 1.77-1.83 (m, 1H), 1.98-2.03 (m, 1H), 2.03-2.05 (t, 1H), 2.64-2.65 (d, $J_{\text{H-H}} = 4$ Hz, 1H), 3.43-3.44 (d, $J_{\text{H-H}} = 4$ Hz, 1H), 6.10 (s-ancho, 1H), 6.89-6.93 (t, 1H), 7.28-7.32 (t, 2H), 7.62-7.65 (d, $J_{\text{H-H}} = 12$ Hz, 2H). ^{13}C $\{^1\text{H}\}$ NMR (101 MHz, CDCl_3): δ 10.64, 13.33, 19.23, 20.30, 20.65, 21.18, 22.07, 27.62, 30.95, 33.84, 47.77, 47.96, 50.22, 51.65, 54.97, 61.37, 63.29, 104.56, 116.51, 120.45, 124.89, 128.46, 128.83, 139.63, 143.41, 166.65. Single crystals suitable for an X-ray analysis were obtained by slow diffusion of hexane into a CH_2Cl_2 solution of **9** at -10°C for two days.

3,3'-((+)-1-phenyl-camphopyrazole)-((+)-2*H*-camphopyrazole) or 3,3'-((4*S*,7*R*)-7,8,8-trimethyl-4,5,6,7-tetrahydro-4,7-methano-1-phenyl-indazol)-((4'*S*,7'*R*)-7',8',8'-trimethyl-4',5',6',7'-tetrahydro-4',7'-methano-2'*H*-indazol) (10**):** Aqueous HCl (12.0 M, 0.50 mL) (0.50 mL) was added dropwise to a solution of **9** (2.50 g, 5.62 mmol) in THF (50.0 mL). The mixture was refluxed overnight. After this time, the solution was washed with saturated aqueous Na_2CO_3 , the organic layer decanted off, dried with MgSO_4 , filtered, and evaporated to an off-white solid (2.04 g, 85 %). Mp 170 – 172°C . $[\alpha]_{\text{D}}^{20} = +170$ (c 0.160, CHCl_3). Elemental analysis calculated for: $\text{C}_{28}\text{H}_{34}\text{N}_4 \cdot 0.5\text{C}_4\text{H}_8\text{O} \cdot 2\text{H}_2\text{O}$ (%): C, 72.26; H, 8.49; N, 11.23. Found: C, 71.93; H, 8.15; N, 11.52. ^1H NMR (400 MHz, CDCl_3): δ 0.74 (s, 3H), 0.83 (s, 3H), 0.93 (s, 3H), 0.96 (s, 3H), 1.12 (s, 3H), 1.24-1.31 (m, 2H), 1.40 (s, 3H), 1.33-1.40 (m, 2H), 1.81 (THF), 1.82-1.88 (m, 2H), 2.10-2.18 (m, 2H), 3.07-3.08 (d, $J_{\text{H-H}} = 4$ Hz, 1H), 3.34-3.35 (d, $J_{\text{H-H}} = 4$ Hz, 1H), 3.71 (THF), 7.33-7.47 (m, 5H), 11.32 (s, 1H). The spectrum indicates the presence of *ca.* 0.5 equiv of THF and 2 equiv of water ^{13}C $\{^1\text{H}\}$ NMR (101 MHz, CDCl_3): δ 10.62, 12.13, 19.31, 19.73, 20.40, 20.59, 27.27, 27.40, 33.77, 33.80, 47.86, 47.91, 50.23, 53.54, 61.00, 63.55, 124.12, 124.48(2), 127.72, 128.04, 128.50, 128.95(2), 136.35, 139.77, 154.94, 167.10.

(+)-3,3'-(1-phenyl-camphopyrazole)-(2-diphenylphosphine-camphopyrazole) or 3,3'-((4*S*,7*R*)-7,8,8-trimethyl-4,5,6,7-tetrahydro-4,7-methano-1-phenyl-indazol)-((4'*S*,7'*R*)-7',8',8'-trimethyl-4',5',6',7'-tetrahydro-4',7'-methano-2'-diphenylphosphine-indazol) (11**):** A cooled solution (-28°C) of LDA (100.9 mg, 0.9418 mmol) in THF (5 mL) was added dropwise over 15 min. to a cooled solution (-28°C) of **10** (400.8 mg, 0.9395 mmol) in THF (10 mL). The resulting dark yellow solution was allowed to warm to RT and was stirred for 2 h. The volatiles were then removed *in vacuo* to afford a beige powder that was redissolved in fresh THF (10 mL) and added dropwise over 10 min to a solution of PPh_2Cl (207.4 mg, 0.9400 mmol) in THF (3 mL). The resulting pale yellow cloudy solution was stirred for 6 h and the evaporated to dryness. The resulting solid was extracted with toluene (10 mL, GF/B filtration). The clear solution was stripped under vacuum to a yellowish solid, which was

washed and slurried with hexane (3 x 10 mL) and HV-dried to afford 500.1 mg (87%) of a white powder. $[\alpha]_D^{20} = +1.36$ (c 0.512, THF). Elemental analysis calculated for $C_{40}H_{43}N_4P \cdot 0.1C_7H_8$ (%): C, 78.85; H, 7.12; N, 9.04. Found: C, 78.75; H, 7.19; N, 9.00. $^{31}P \{^1H\}$ RMN (162 MHz, CD_2Cl_2): δ 45.96 s (1P). 1H RMN (400 MHz, CD_2Cl_2): δ 7.31 – 7.64 (m, 15H), 3.05 (d, $J = 3.30$ Hz, 1H), 2.96 (d, $J = 3.66$ Hz, 1H), 2.04 (m, 2H), 1.78 (m, 2H), 2.32 (m, 1H), 2.12 (m, 1H), 1.47 (s, 3H), 1.25 – 1.36 (m, 1H), 1.15 (s, 3H), 0.93 (s, 3H), 0.91 (s, 3H), 0.83 (s, 3H), 0.82 (s, 3H). The spectrum shows 11 mol% of co-crystallized toluene. ^{13}C RMN $\{^1H\}$ (101 MHz, CD_2Cl_2): δ 163.6 (d, $^2J_{C-P} = 18.90$ Hz, C), 154.1 (C), 144.3 (C), 140.5 (d, $^3J_{C-P} = 12.15$ Hz, 2C), 138.1 (d, $^3J_{C-P} = 9.45$ Hz, C), 137.5 (d, $^3J_{C-P} = 9.45$ Hz, C), 135.4 (d, $^3J_{C-P} = 6.75$ Hz, C), 135.2 (d, $^3J_{C-P} = 6.75$ Hz, C), 133.7 (CH), 133.5 (CH), 132.7 (CH), 132.5 (CH), 129.8 (CH), 129.5 (CH), 128.7(2CH), 128.3 (CH), 128.2 (2CH), 128.1 (CH), 127.1 (CH), 124.3(2CH), 62.9 (CH), 62.6 (CH), 53.7 (CH), 53.6 (CH), 48.3 (CH), 48.2 (CH), 33.9 (CH₂), 33.8 (CH₂), 27.5 (CH₂), 27.2 (CH₂), 20.2 (CH₃), 20.2 (CH₃), 19.6 (CH₃), 19.5 (CH₃), 12.3 (CH₃), 12.2 (CH₃).

General protocol for the preparation of nickel complexes. A 0.1 M solution of ligand in THF was added slowly to a stirred 0.1 M suspension of the metal halide solvate in THF and the reaction mixture was stirred at room temperature for 18 h. The resulting precipitate was separated from the supernatant solution by decantation, washed with several portions of hexane, and dried *in vacuo* for 4 h.

[NiBr₂(3)] (12): Ligand **3** (325 mg, 0.84 mmol) and NiBr₂(THF)₂ (296 mg, 0.82 mmol). Recrystallized from THF-hexane mixture (1:1). Purple solid (430 mg, 84 %). Elemental analysis calculated for $C_{24}H_{28}Br_2N_4NiO$ (%): C, 47.49; H, 4.65; N, 9.23. Found: C, 47.51; H, 4.65; N, 9.28. X-ray quality single crystals of **12** were obtained by slow diffusion of hexane into a saturated solution of **7** in THF and cooling to -10 °C for 2 d.

[NiBr₂(4)] (13): Ligand **4** (365 mg, 0.79 mmol) and NiBr₂(THF)₂ (283 mg, 0.77 mmol). Recrystallized from THF-hexane mixture (1:1). Green solid (499 mg, 96 %). Elemental analysis calculated for $C_{29}H_{38}Br_2N_4NiO \cdot 3H_2O$: C, 47.64; H, 6.07; N, 7.66. Found: C, 47.48; H, 6.37; N, 7.47.

[NiBr₂(6)] (14): Ligand **6** (311 mg, 0.62 mmol) and NiBr₂(THF)₂ (225 mg, 0.62 mmol). Grey solid product (380 mg, 85 %). Elemental analysis calculated for $C_{34}H_{38}Br_2N_4Ni$ (%): C, 56.62; H, 5.31; N, 7.77. Found: C, 56.35; H, 5.48; N, 7.53. Slow evaporation at room temperature of a saturated solution of **14** in THF afforded crystals suitable for X-ray diffraction.

[PdCl₂(6)] (15): Ligand **6** (250 mg, 0.50 mmol) and PdCl₂(CH₃CN)₂ (129 mg, 0.50 mmol). Orange solid product (279 mg, 82 %). Elemental analysis calculated for $C_{34}H_{38}Cl_2N_4Pd \cdot 2.5H_2O$ (%): C, 56.32; H, 5.98; N, 7.73. Found: C, 56.04; H, 5.39; N, 7.45. 1H NMR (400 MHz, $CDCl_3$): δ 0.83 (s, 6H), 0.88 (s, 6H), 0.94 (s, 6H), 1.25-1.30 (m, 4H), 1.81-1.86 (m, 2H), 2.17-2.22 (m, 2H), 3.00-3.01 (d, $J_{H-H} = 4$

Hz, 2H), 7.38-7.42 (m, 10H). ^{13}C $\{^1\text{H}\}$ NMR (101 MHz, CDCl_3): δ 11.16, 19.26, 20.34, 27.08, 33.37, 47.90, 54.42, 63.18, 125.48, 127.19 (2), 128.61 (2), 129.76, 137.24, 139.52, 159.77.

[RhCl(11)(PPh₂Cl)] (16): A benzene (1.5 mL) solution of ligand **2** (101.4 mg, 0.166 mmol) was added to a suspension of $[\text{RhCl}(\text{COD})]_2$ (40.9 mg, 0.0829 mmol) in benzene (0.5 mL). The resulting dark orange solution was stirred for 4 h and then evaporated to dryness to afford a yellow solid. Washing with hexane (3 x 5 mL) yielded 69 mg (86%) of a light orange powder. Elemental analysis calculated for $\text{C}_{32}\text{H}_{53}\text{N}_4\text{P}_2\text{Cl}_2\text{Rh}$ (%): N 5.78, C 64.40, H 5.51. Found: N 5.82, C 64.61, H 5.76. ^{31}P $\{^1\text{H}\}$ NMR (162 MHz, C_6D_6): δ 130.83 (dd, $^1J = 223.3$ Hz, $^2J = 41.7$ Hz, 1P), 100.70 (dd, $^1J = 195.0$ Hz, $^2J = 41.7$ Hz, 1P). ^1H NMR (400 MHz, C_6D_6): δ 7.70 - 8.31 (m, 10H), 7.33 - 7.39 (m, 2H), 7.25 - 7.31 (m, 1H), 6.81 - 7.12 (m, 12H), 3.01 (d, $J = 3.61$ Hz, 1H), 2.95 (d, $J = 3.19$ Hz, 1H), 1.90 (m, 1H), 1.72 (m, 1H), 1.60 (m, 1H), 1.38 (m, 1H), 1.17 - 1.31 (m, 2H), 1.05 (s, 3H), 0.81-0.91 (m, 2H), 0.61-0.80 (m, 12H), 0.51 (s, 3H). Crystals suitable for X-ray diffraction were obtained by layering hexane (3 mL) onto a 10 % w/w filtered solution of **16** in CH_2Cl_2 (0.5 mL) and cooling to -27°C for 3 d.

Crystal structure determinations: The measurements for **1**, **6**, **7**, and **12** were made on a Rigaku AFC-7 diffractometer equipped with a Mercury CCD area-detector using graphite-monochromated Mo $K\alpha$ radiation ($\lambda = 0.71073$ Å). The intensities were corrected for Lorentz and polarization effects, and an absorption correction based on the multi-scan method was applied by using *CrystalClear*.²⁶ The space group was uniquely determined by the systematic absences. Equivalent reflections were merged. The data for compounds **8** and **14** were collected on a Bruker-Nonius KappaCCD area-detector diffractometer²⁷ using graphite-monochromated Mo $K\alpha$ radiation, and data reduction was performed with *EvalCCD*.²⁸ The data for compound **16** were collected on a Bruker Kappa APEX 2 $I\mu\text{S}$ Duo diffractometer²⁹ using Mo $K\alpha$ radiation with QUAZAR focussing Montel optics and APEX2²⁹ for data reduction. The measurements for compound **9** were conducted on an Oxford Diffraction SuperNova area-detector diffractometer using Mo $K\alpha$ radiation and an Oxford Instruments Cryojet cooler, and data reduction was performed with *CrysAlisPro*.³⁰ All the structures were solved by direct methods using *SHELXS-97*³¹, *SHELXS-2013*³¹ or *SHELXTL*³² and the non-hydrogen atoms were refined anisotropically. All refinements were carried out using *SHELXL-97*³¹, *SHELXL-20*³³ or *SHELXTL*³². The data collection and refinement parameters are given in Table 1.

The asymmetric unit of **1** and **7** contains two crystallographic independent molecules of the same enantiomer. In compound **1**, the acidic protons HO1 and HO3 were located from a difference Fourier map, which were included by restraints in the O–H distances. Compound **8** crystallized with two independent molecules in the asymmetric unit representing the same enantiomer. H atoms were treated

as follows: The positions of the two O-bound H atoms H01O1 and H03O3 were taken from a difference Fourier synthesis and refined. Structure **12** crystallized with two independent metal complexes and two THF molecules in the asymmetric unit. Both solvent molecules were found disordered over two sets of positions, which were included by restraints in the C–C and C–O distances and complementary occupancies of 63:37 and 57:43, respectively. These atoms were refined anisotropically. For structure **14**, similarity restraints were applied to the atomic displacement parameters during the refinement of the disordered Br atoms. The crystal under study was an inversion twin with a major twin fraction of 0.851(7) (see Flack parameter).

CCDC 1477566–1477573 contain the supplementary crystallographic data for this paper. The data can be obtained free of charge from The Cambridge Crystallographic Data Centre via www.ccdc.cam.ac.uk/getstructures.

Acknowledgements

This work was funded by FONACIT (project S1-2001000851) and DID–USB (project S1–IN–CB–005–12). We thank Ms. Eleinne Severino (IVIC) for carrying out the elemental analyses.

References

-
- ¹ For camphor-derived functional chiral ionic liquids, see: (a) Pastrán, J.; Agrifoglio, G.; González, T.; Briceño, A.; Dorta, R. *Tetrahedron: Asymmetry* **2014**, *25*, 1280; For a recent review on camphor-derived organo-catalysts, see: (b) Grošelj, U. *Current Org. Chem.* **2015**, *19*, 2048.
- ² For the X-ray crystal structure, see: Llamas-Saiz, A.; Foces-Foces, C.; Sobrados, I.; Elguero, J.; Meutermans, W. *Acta Crystallogr., Sect. C: Cryst. Struct. Commun.*, **1993**, *49*, 724.
- ³ (a) Steel, P. *Acta Cryst.* **1983**, *C39*, 1623; (b) House, D. A.; Steel, P.; Watson, A. A. *Aust. J. Chem.* **1986**, *39*, 1525; (c) Watson, A. A.; House, D. A.; Steel, P. *Aust. J. Chem.* **1995**, *48*, 1549. For the luminescent properties of Pt complexes bearing such ligands, see: (d) Kavitha, J.; Chang, S. Y.; Chi, Y.; Yu, J. K.; Hu, Y. H.; Chou, P. T.; Peng, S. M.; Lee, G. H.; Tao, T. T.; Chien, C. H.; Carty, A. J. *Adv. Funct. Mater.* **2005**, *15*, 223; (e) Chang, S. Y.; Kavitha, J.; Hung J. Y.; Chi, Y. *Inorg. Chem.* **2007**, *46*, 7064. For ligands containing two and three camphopyrazole units, see: (f) LeCloux, D. D.; Tokar, C. J.; Osawa, M.; Houser, R. P.; Keyes, M. C.; Tolman, W. B. *Organometallics* **1994**, *13*, 2855; (g) Kashima, C.; Miwa, Y.; Shibata, S.; Nakazono, H. *J. Heterocyclic Chem.* **2003**, *40*, 681; (h) Elflein, J.; Platzmann, F.; Burzlaff, N. *Eur. J. Inorg. Chem.* **2007**, 5173; (i) Godau, T.; Bleifub, S. M.; Muller, A. L.; Roth, T.; Hoffmann, S.; Heinemann, F. W.; Burzlaff, N. *Dalton Trans.* **2011**, *40*, 6547.

-
- ⁴ (a) Spallek, M.; Stockinger S.; Goddard, R.; Rominger, F.; Trapp, O. *Eur. J. Inorg. Chem.* **2011**, 5014-5024; (b) Spallek, M.; Stockinger S.; Goddard, R.; Trapp, O. *Adv. Synth. Catal.* **2012**, 354, 1466.
- ⁵ (a) Suzuki, Y.; Ogata, Y.; Hiroi, K. *Tetrahedron: Asymmetry* **1999**, 10, 1219; (b) Chelucci, G.; Saba, A.; Socolini, F. *Tetrahedron* **2001**, 57, 9989; (c) Malaisé, G.; Barloy, L.; Osborne, J. A. *Tetrahedron Lett.* **2001**, 42, 7417; (d) Bunlaksananusorn, T.; Polborn, K.; Knochel, P. *Angew. Chem. Int. Ed.* **2003**, 115, 4071; (d) Bunlaksananusorn, T.; Pérez Luna, A.; Bonin, M.; Micouin, L.; Knochel, P. *Synlett* **2003**, 14, 2240; (e) Ilaldinov, I.; Fatkulina, D.; Bucharov, S.; Jackstell, R.; Spannenberg, A.; Beller, M.; Kadyrov, R. *Tetrahedron: Asymmetry* **2011**, 22, 1936.
- ⁶ Alcock, N.W.; Brown, J.M.; Hulmes, D.I. *Tetrahedron: Asymmetry* **1993**, 4, 743.
- ⁷ For reviews: (a) P. J. Guiry and C. P. Saunders, *Adv. Synth. Catal.* **2004**, 346, 497; (b) D. Amoroso, T. W. Graham, R. Guo, C.-W. Tsang and K. Abdur-Rashid, *Aldrichimica Acta*, **2008**, 41, 15; (c) I. D. Kostas, *Curr. Org. Synth.*, **2008**, 5, 227. For recent examples of chiral P-pyrazoles, see: (d) Willms, H.; Frank, W.; Ganter, C. *Organometallics* **2009**, 28, 3049.
- ⁸ Chiral Rh(I)-(P,N) complexes may serve as catalyst for enantioselective hydrogenation or C–C bond forming reactions, and chiral Ni(II)-(N,N) complexes may be stereoselective polymerization catalysts. See for example: (a) Rose, J. M.; Cherian, A. E.; Coates, G. W. *J. Am. Chem. Soc.* **2006**, 128, 4186; (b) Yuan, J.; Wang, F.; Xu, W.; Mei, T.; Li, J.; Yuan, B.; Song, F.; Jia, Z. *Organometallics* **2013**, 32, 3960 and references cited therein.
- ⁹ Noe, C. R.; Knollmüller, M.; Gärtner, P.; Mereiter, K.; Steinbauer, G. *Liebigs. Ann.* **1996**, 1015.
- ¹⁰ Nagai, S.; Oda, N.; Ito, I.; Kudo, Y. *Chem. Pharm. Bull.* **1979**, 27, 1771.
- ¹¹ Gerlach, H.; Kappes, D.; Boeckman, R. K.; Maw, G. N. *Org. Synth.* **1998**, 9, 151.
- ¹² (a) Hart, I. J. *Polyhedron* **1992**, 11, 729; (b) T. M. Shironina, N. M. Igidov, E. N. Koz'minykh, L. O. Kon'shina, Y. S. Kasatkina, V. O. Koz'minykh, *Russ. J. Org. Chem.* **2001**, 37, 1486.
- ¹³ Depending on the purity of reagents and solvents used for this reaction, a minor byproduct may form, showing a characteristic singlet at 45.7 ppm in the ³¹P NMR spectrum. We believe this to be the isomer with the PPh₂ moiety attached to the neighboring N atom of the pyrazol ring. The high selectivity for **11** is probably due to bidentate coordination of Li in deprotonated **10** followed by a regioselective reaction with the PPh₂Cl electrophile.
- ¹⁴ Pandarus, V.; Zargarian, D. *Organometallics* **2007**, 26, 4321.
- ¹⁵ Doyle, J. R.; Slade, P. E.; Jonassen, H. B. *Inorg. Synth.* **1960**, 6, 218.

-
- ¹⁶ Feldman, J.; McLain, S. J.; Parthasarathy, A.; Marshall, W. J.; Calabrese, J. C.; Arthur, S. D. *Organometallics* **1997**, *16*, 1514.
- ¹⁷ Hitchcock, P. B.; Lee, T. H.; Leigh, G. J. *Inorg. Chim. Acta* **2003**, *355*, 168.
- ¹⁸ For similar reactions of pyrazolylphosphines with BCl₃, see: (a) Fischer, S.; Hoyano, J.; Peterson, L. K. *Can. J. Chem.* **1976**, *54*, 2710. In order to prevent P–N bond cleavage in such ligands, chloride free metal precursors may be employed: (b) Tazelaar, C. G. J.; Lyakovskyy, V.; van Doorn, I. M.; Schaapkens, X.; Lutz, M.; Ehlers, A. W.; Slootweg, J. C.; Lammertsma, K. *Eur. J. Inorg. Chem.* **2013**, 1836; (c) Tazelaar, C. G. J.; Nicolas, E.; van Dijk, T.; Broere, D. L. J.; Cardol, M.; Lutz, M.; Gudat, D.; Slootweg, J. C.; Lammertsma, K. *Dalton Trans.* **2016**, *45*, 2237.
- ¹⁹ ¹H NMR data of *in situ* reaction mixtures show *ca.* 1 equiv of free COD plus 1 equiv of what appears to be a Rh(COD)-complex bearing anionic **10** as a bidentate ligand.
- ²⁰ Janiak, C. *J. Chem. Soc. Dalton Trans.* **2000**, 3885.
- ²¹ Muñoz, S.; Pons, J.; Solans, X.; Font-Bardia, M.; Ros, J. *J. Organomet. Chem.* **2008**, *693*, 2132.
- ²² Alock, N.; Brown, J.; Hulmes, D. *Tetrahedron: Asymmetry* **1993**, *4*, 743.
- ²³ Noe, C. R.; Knollmüller, M.; Gärtner, P.; Mereiter, K.; Steinbauer, G. *Liebigs. Ann.* **1996**, 1015.
- ²⁴ Barnett, N.; Mulvey, R. *J. Am. Chem. Soc.* **1991**, *113*, 8187.
- ²⁵ Giordano, G.; Crabtree, R. H. *Inorganic Synthesis* **1990**, *28*, 88.
- ²⁶ *CrystalClear*, version 1.3.6; Rigaku MSC, Inc.: The Woodlands, TX, 200.
- ²⁷ *COLLECT*, Bruker AXS BV, Delft, The Netherlands, **2002**.
- ²⁸ A. J. M. Duisenberg, L. M. J. Kroon-Batenburg & A. M. M. Schreurs, *J. Appl. Cryst.* **2003**, *36*, 220.
- ²⁹ *APEX2*, Version 2014.9-0, Bruker AXS, Madison, WI, U.S.A., **2014**.
- ³⁰ CrysAlisPro, Oxford Diffraction Ltd., Version 1.171.33.55, **2010**.
- ³¹ G. M. Sheldrick, *Acta Crystallogr., Sect. A*, **2008**, *64*, 112.
- ³² *SHELXTL* Version 6.12, Bruker AXS, Madison, WI, U.S.A., **2002**.
- ³³ G. M. Sheldrick, *Acta Crystallogr., Sect. C*, **2015**, *71*, 3.

Table 1. Crystallographic data for compounds **1**, **6–9**, **12**, **14**, and **16**

	1	6	7	8	9	12	14	16
Empirical formula	C ₃₆ H ₃₈ N ₄ O ₄	C ₃₄ H ₃₈ N ₄	C ₄₈ H ₁₀ N ₄ O ₄	C ₂₈ H ₃₄ N ₂ O ₂	C ₂₈ H ₃₇ N ₄ O _{0.5}	C ₂₄ H ₂₉ Br ₂ N ₄ NiO	C ₃₄ H ₃₈ Br ₂ N ₄ Ni	C ₅₃ H ₅₅ Cl ₄ N ₄ P ₂ Rh
Formula weight	590.70	502.68	706.60	430.57	453.63	608.04	721.21	1054.66
Crystal System	Monoclinic	Monoclinic	Orthorhombic	Triclinic	Orthorhombic	Triclinic	Monoclinic	Triclinic
Space group	<i>P</i> 2 ₁	<i>P</i> 2 ₁	<i>P</i> 2 ₁ 2 ₁ 2 ₁	<i>P</i> 1	<i>P</i> 2 ₁ 2 ₁ 2 ₁	<i>P</i> 1	<i>P</i> 2 ₁	<i>P</i> 1
Temperature (K)	293	293	293	150	100	293	150	100
<i>a</i> (Å)	12.5256(18)	7.333(5)	11.040(4)	6.7124(3)	13.17868(16)	9.223(5)	10.2647(11)	11.735(2)
<i>b</i> (Å)	6.9042(10)	19.593(13)	13.819(5)	7.8719(2)	16.2917(2)	13.743(10)	21.107(3)	13.034(2)
<i>c</i> (Å)	19.193(3)	9.950(7)	17.884(6)	22.1268(9)	24.7251(3)	13.752(9)	14.5382(6)	17.062(2)
α (°)	90	90	90	91.525(3)	90	113.004(11)	90	75.921(3)
β (°)	90.170(3)	93.161(19)	90	91.674(4)	90	92.511(12)	92.556(6)	82.045(3)
γ (°)	90	90	90	91.353(3)	90	103.529(12)	90	77.452(3)
V(Å ³)	1659.8(4)	1427.4(16)	2728.5(15)	1167.90(8)	5308.11(11)	1542.1(17)	3146.7(6)	2460.6(5)
<i>Z</i>	2	2	3	2	8	2	4	2
Reflections collected/unique	19113/5871	14714/5039	32025/5132	36991/5143	54496/10819	17206/10195	90257/14957	87766/22899
Reflns observed [<i>I</i> > 2 σ (<i>I</i>)]	2873	2832	3504	4730	9285	7211	13372	21035
<i>R</i> (int)	0.072	0.071	0.056	0.045	0.025	0.026	0.050	0.036
Restraints/parameters	1/397	1/344	0/317	3/595	0/633	3/618	13/772	3/1153
<i>R</i> (<i>F</i>) [<i>I</i> > 2 σ (<i>I</i>) reflns]	0.068	0.080	0.061	0.038	0.036	0.060	0.036	0.028
<i>wR</i> (<i>F</i> ²) (all data)	0.196	0.202	0.190	0.092	0.092	0.204	0.085	0.069
Goodness-of-fit on <i>F</i> ²	1.08	1.06	1.15	1.08	1.05	1.20	1.08	1.03
Max./min. $\Delta\rho$ (e Å ⁻³)	0.20/-0.29	0.18/-0.20	0.23/-0.18	0.20/-0.25	0.25/-0.18	0.67/-0.59	0.49/-0.61	0.46/-0.54